LETTER

doi:10.1038/nature09697

Hard-tip, soft-spring lithography

Wooyoung Shim[1,2], Adam B. Braunschweig[2,3]†, Xing Liao[1,2], Jinan Chai[2,3], Jong Kuk Lim[2,3], Gengfeng Zheng[2,3]† & Chad A. Mirkin[1,2,3]

Nanofabrication strategies are becoming increasingly expensive and equipment-intensive, and consequently less accessible to researchers. As an alternative, scanning probe lithography has become a popular means of preparing nanoscale structures, in part owing to its relatively low cost and high resolution, and a registration accuracy that exceeds most existing technologies[1–6]. However, increasing the throughput of cantilever-based scanning probe systems while maintaining their resolution and registration advantages has from the outset been a significant challenge[7–17]. Even with impressive recent advances in cantilever array design, such arrays tend to be highly specialized for a given application, expensive, and often difficult to implement. It is therefore difficult to imagine commercially viable production methods based on scanning probe systems that rely on conventional cantilevers. Here we describe a low-cost and scalable cantilever-free tip-based nanopatterning method that uses an array of hard silicon tips mounted onto an elastomeric backing. This method—which we term hard-tip, soft-spring lithography—overcomes the throughput problems of cantilever-based scanning probe systems and the resolution limits imposed by the use of elastomeric stamps and tips: it is capable of delivering materials or energy to a surface to create arbitrary patterns of features with sub-50-nm resolution over centimetre-scale areas. We argue that hard-tip, soft-spring lithography is a versatile nanolithography strategy that should be widely adopted by academic and industrial researchers for rapid prototyping applications.

Molecular printing capabilities[1], where molecules and materials can be directly delivered to a surface in the form of nanometre-scale features, have been dramatically accelerated through the invention of micro-contact printing[18,19] and dip-pen nanolithography[2,20], two micro- and nanofabrication techniques that have complementary strengths and weaknesses. The former allows a master to be duplicated repeatedly over large areas with 200-nm resolution in a rapid fashion[21,22]. It is limited with respect to registration, requires a mask for every new master, and is not well-suited for making closely spaced structures with different chemical inks. The latter provides sub-50-nm resolution, custom nanostructure generation capabilities, high registration capabilities, and with cantilever arrays, a modest ability to generate structures made of different chemical compositions simultaneously[23,24]. It does not have the throughput of contact printing and requires substantially higher cost and cumbersome cantilever array technology. Attempts to combine the capabilities of dip-pen nanolithography and micro-contact printing have led to the development of polymer pen lithography[25,26], a low cost scanning probe approach that utilizes an elastomeric stamp made of pyramids to generate arbitrary patterns over surfaces by using the tips of the pyramids as compressible point sources of molecules or materials to be delivered to an underlying substrate. Polymer pen lithography is a significant advance in that it eliminates most of the drawbacks of the two techniques and combines almost all of their attributes. However, it does not offer the sub-50-nm resolution[25] afforded by high resolution scanning probe lithography or alternative electron-beam technologies.

Ideally, one would like an array of hard tips resting on springs made of soft materials to create a technique that provides the high resolution of a single-tip scanning probe lithography experiment and the scalability of polymer pen lithography. Here we describe a new tip array architecture that achieves this goal and provides a way of engaging and aligning as many as 4,750 ultrasharp Si tips on a surface over an area of one square centimetre (in principle, the arrays could be much larger).

Major advances in scanning probe lithography are often the result of novel tip designs and fabrication procedures. The key innovation that enables hard-tip, soft-spring lithography (HSL) is a new protocol for fabricating arrays of ultra-sharp Si tips on a spring-like elastomer layer that allows all of the tips to be brought into contact with a surface over large areas (Fig. 1a). The HSL tip array architecture is composed of thousands of Si tips attached to a layer of elastomer that coats a glass slide. The elastomeric backing significantly reduces the cost of fabrication because it circumvents the necessity for micromachined cantilevers, and enables a levelling protocol without requiring a complex feedback scheme[26]. The Si tips, prepared by an established self-sharpening wet etching protocol[27], have an average diameter of 22 ± 3 nm. Because the tip arrays are prepared on a glass slide, they can be easily mounted onto the piezoelectric actuators of a conventional atomic force microscope, which provides precise tip positioning and registration, hallmarks of scanning probe lithographies. Both the elastomer and the glass onto which the arrays are mounted are transparent, which enables the visual observation of the compression of the elastomer that occurs when the tips touch the surface of a substrate (see Supplementary Video 1), thereby enabling a straightforward, optical method for levelling the plane of the tip array with respect to the substrate surface.

Depending on the intended use, the pitch of a tip array is deliberately set between 100 and 200 μm, corresponding to tip densities of 10,000 cm^{-2} and 2,500 cm^{-2}, respectively, and the density can be as high as 110,000 cm^{-2} (9,007,700 tips in 4-inch wafer) with a pitch of 30 μm. To make the tip arrays (Fig. 1b), a 1 cm × 1 cm piece of a 50-μm-thick (100)Si wafer with a 1-μm-thick layer of SiO_2 on each side of the wafer was placed onto the uncured elastomer. The top layer of the SiO_2 eventually serves as an etching mask, while the oxygen-plasma-treated bottom SiO_2 layer of the wafer in contact with the hydrophilic surface of the elastomer increases adhesion between the two surfaces, so that the tips do not fall off the array once the wafer has been etched (Supplementary Fig. 1). Following the curing of the elastomer, photolithography was used to define 150 μm × 150 μm square features of exposed SiO_2, each of which can be used to prepare an ultrasharp tip. HF is used to remove the exposed SiO_2, and aqueous KOH (40% w/v) is used to anisotropically etch the underlying Si. An array of square SiO_2 masks along the <110> direction exposes the (311) and (100) planes of the wafer during KOH etching at rates of 88 and 50 μm h^{-1}, respectively. To achieve self-sharpening, $R_w/\cos\theta$ (where R_w is the sidewall etching rate and θ is the slope of the tip sidewall) must exceed the surface etching rate, R_f (ref. 27). Thus the critical anisotropy ratio η_c and the condition for self-sharpening η are

[1]Department of Materials Science and Engineering, Northwestern University, 2220 Campus Drive, Evanston, Illinois 60208, USA. [2]International Institute for Nanotechnology, Northwestern University, 2145 Sheridan Road, Evanston, Illinois 60208, USA. [3]Department of Chemistry, Northwestern University, 2145 Sheridan Road, Evanston, Illinois 60208, USA. †Present addresses: Department of Chemistry, New York University, 100 Washington Square East, New York, New York 10003, USA (A.B.B.); Laboratory of Advanced Materials & Department of Chemistry, Fudan University, 2205 Song-Hu Road, Shanghai, 200438, China (G.Z.).

©2011 Macmillan Publishers Limited. All rights reserved

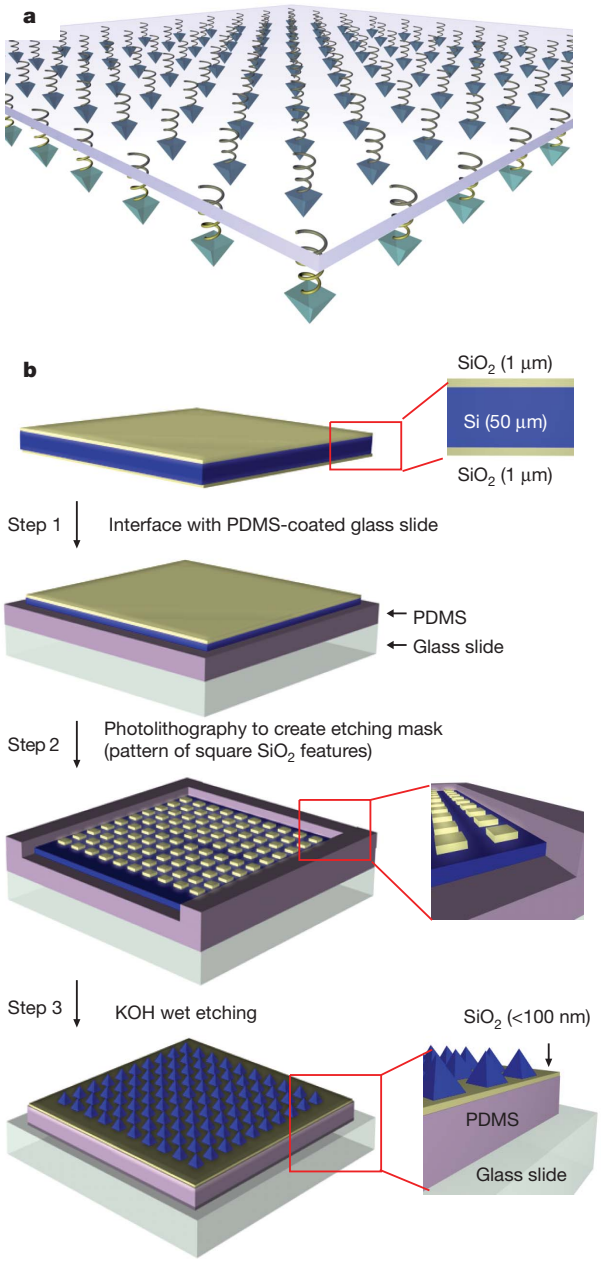

Figure 1 | Fabrication of an HSL tip array. **a**, Schematic illustration of an HSL tip array supported by a transparent, soft backing layer that provides mechanical flexibility to each tip. **b**, Experimental procedure to fabricate the tip arrays: 50-μm-thick (100)Si wafers with thermally oxidized SiO_2 (1-μm thick) on each side were used. Step 1, an oxygen-plasma-treated Si wafer is placed onto uncured polydimethylsiloxane (PDMS) on a glass slide, followed by curing. Step 2, an array of square SiO_2 masks of different edge lengths (100–200 μm with 5 μm separation) along the <110> direction is defined by conventional photolithography and an isotropic buffered hydrofluoric acid (HF) etch. An additional PDMS passivation layer on the edge of the Si wafer protects the sides of the wafer from exposure to the etching solution, thereby preventing the (110) crystal face on the sides of the wafer from etching faster than the (100) face on the surface. Step 3, the arrays of tips are formed by etching the Si in a 40 wt% KOH (aq.) solution at 75 °C. After a defined time (60–65 min) when the sample became transparent owing to the removal of the opaque Si, the sample was removed from the etchant, rinsed with water, dried using a nitrogen stream, and if necessary, further SiO_2 etching was conducted in HF to increase the flexibility of the backing layer.

expressed as $\eta = R_f/R_w \leq 1/\cos\theta = \eta_c$, which indicates that sidewall etching must be faster than etching of the tip base in order to form a sharp tip. For the HSL tip array made here, the experimental $\eta = R_{(100)}/R_{(311)}$ is 0.56 in 40 wt% KOH at 75 °C, while the theoretical η_c required for self-sharpening conditions is 3.33 (ref. 27).

Optical and scanning electron microscopy (SEM) analysis of the resulting tip arrays reveal that this fabrication protocol does, indeed, yield an array of uniform Si nanotips (Fig. 2). The Si wafer, before KOH etching, is immobilized onto a glass slide using uncured polydimethylsiloxane (PDMS; Fig. 2a); curing results in adhesion and the generation of a rigid support for the Si substrate and eventually the tip array, which is made from the KOH etching procedure. This protocol allows one to handle and manipulate the fragile tip array without damaging it, and the glass-supported structure serves as a platform that can be easily mounted onto an AFM scanner. The glass-supported tip array is transparent (Fig. 2b), which enables the visual levelling of the tips with respect to a surface. An SEM image of the tips with a 150 μm centre-to-centre separation shows that they adhere well to the elastomer surface and are remarkably uniform, with an average bottom diameter of 30 ± 0.6 μm (Supplementary Fig. 2) and an average tip height of 47 ± 0.9 μm (Fig. 2c). The tip height variation may cause a few tens of milliseconds difference in contact time between a tip and the surface, but not vary the feature size significantly. SEM analysis also shows that the surface intersection angles, α_1 and α_2, and the rotation of the intersection of the planes to the <100> direction of the wafer, φ, are 127°, 143° and 18° (Fig. 2d), respectively, which shows that the sidewalls of the tips are (311) planes; indeed the angle values correspond well with the theoretical values of the intersection angles for (311) planes of Si, which are 126.9°, 143.1° and 18.4°, respectively[27]. Importantly, this procedure results in a tip yield >99%, and the average Si tip diameter is 22 ± 3 nm (Fig. 2e), demonstrating that self-sharpening

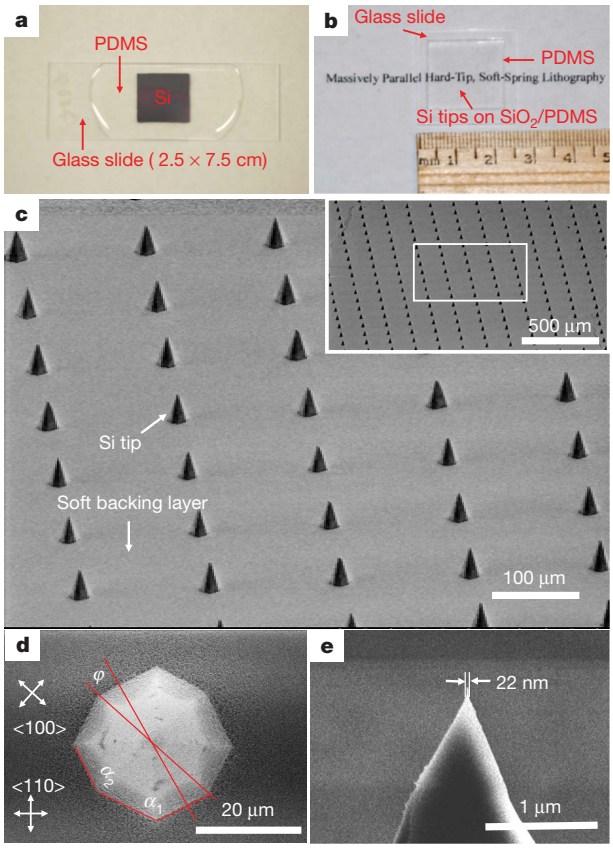

Figure 2 | HSL tip arrays. **a**, Si wafer (2 × 2 cm) on a cured PDMS surface rests on a glass slide before KOH etching. **b**, A transparent Si tip array after etching in KOH. **c**, An SEM image of the Si tip array on SiO_2/PDMS/glass with a 150-μm pitch between tips. The inset shows a large area of the array to demonstrate the homogeneity of the tips. **d**, The (311) planes of Si were exposed during the wet etching with [110] oriented masks on a (100)Si surface. **e**, SEM image of a tip with diameter 22 nm.

©2011 Macmillan Publishers Limited. All rights reserved

has been realized. Note that the tip diameter, in principle, could be reduced down to 5 nm by optimizing etching conditions[28], but these tips are sufficient to evaluate the potential for sub-50-nm lithography. Finally, because the wafer thickness has a variation of ~10% (50 ± 5 μm, NOVA Electronic Materials), the tip height can also vary up to 10%.

The molecular printing capabilities of HSL—including the ability to make arbitrary patterns, reproducibility, and time-dependent feature size control—were evaluated in the context of printing poly(ethylene glycol) (PEG) and 16-mercaptohexadecanoic acid (MHA) onto a hexamethyldisilazane-coated Si surface and a thermally evaporated polycrystalline Au surface, respectively. The tip arrays were inked by spin-coating an ethanol solution of PEG or MHA onto the tip arrays, which were subsequently mounted onto an XE-150 AFM platform (Park Systems) that was specially equipped with a tilt stage, an environmental humidity control chamber, a specialized scanning head (Fig. 3a), and lithography software capable of controlling the position, dwell time, and vertical-axis piezo (*z*-piezo) extension for each feature in a pattern. In a departure from dip-pen nanolithography and all cantilever-based lithography approaches, there is no need for laser feedback during writing: rather, the compression of the elastomer backing as the tips push against the surface is used to indicate that the tips are in contact with the surface and that writing is occurring (Fig. 3b and Supplementary Fig. 3). This optical signal is also used to level the plane of the tip array with respect to the plane of the surface: the tilt angle of the tip array is adjusted until, upon *z*-piezo extension, all of the tips contact the surface (see Supplementary Video 1 of the tips being aligned). As a way of evaluating the resiliency of the tip architecture, the *z*-motor was extended as far as 100 μm after the tips have touched the surface, and the array structure was subsequently analysed. Significantly, upon retraction the tips rebound without breaking off the support (see Supplementary Video 2).

In polymer pen lithography, there is a linear relationship between the force between the tip array and the surface and the resulting feature edge length because of the compression of the polymeric tips[25], however in HSL, no such relationship is observed because the Si tips do not deform under pressure. PEG was written with a dwell time of 0.5 s, at a humidity of 80%, and with *z*-piezo extension values ranging from 4 to 12 μm without any significant deviation in the size of the features (564 ± 23 nm) written by any single tip (Fig. 3c and d). This lack of feature diameter dependence on the force exerted between the tip array and the surface suggests that all tips in HSL can be brought into contact with a surface by extending the *z*-piezo without consequences on the resulting feature sizes, even though the force exerted on each tip may differ. In dip-pen nanolithography, precise control of feature diameter is achieved because the ink diffuses through the meniscus that forms between the tip and the surface, thereby resulting in a linear relationship between feature area A and the square root of the dwell time t, $A \propto \sqrt{t}$ (ref. 23). This relationship between feature and dwell time was investigated in the context of an HSL experiment by writing an MHA pattern on an Au polycrystalline surface, and varying the feature dwell times. The dots were written at dwell times from 1 to 15 s at 50% humidity and resulted in etched Au features with diameters from 261 ± 22 to 1,002 ± 32 nm, respectively (Fig. 3e), showing that this linear relationship is maintained (Fig. 3d), although there seems to be a saturation of feature size above dwell times of 13 s. When the humidity is lowered to 15%, etched Au dot features with diameters as small as 34 ± 5 nm can be reproducibly obtained with a dwell time of 0.01 s (Fig. 3f; also see Supplementary Fig. 4 for an MHA pattern on Au), showing that dwell time and humidity can be used to effectively control the resulting feature size from several micrometres to less than 50 nm (Fig. 3d).

The ability to use the HSL tip arrays to transfer energy, rather than materials (ink), to a surface was also evaluated (Supplementary Fig. 5). For example, HSL was used to make a pattern of holes in a 30-nm-thick PMMA film. The tip arrays were lowered into the polymer at 30% humidity and a 0.5 s contact time, which resulted in 38 ± 4 nm diameter

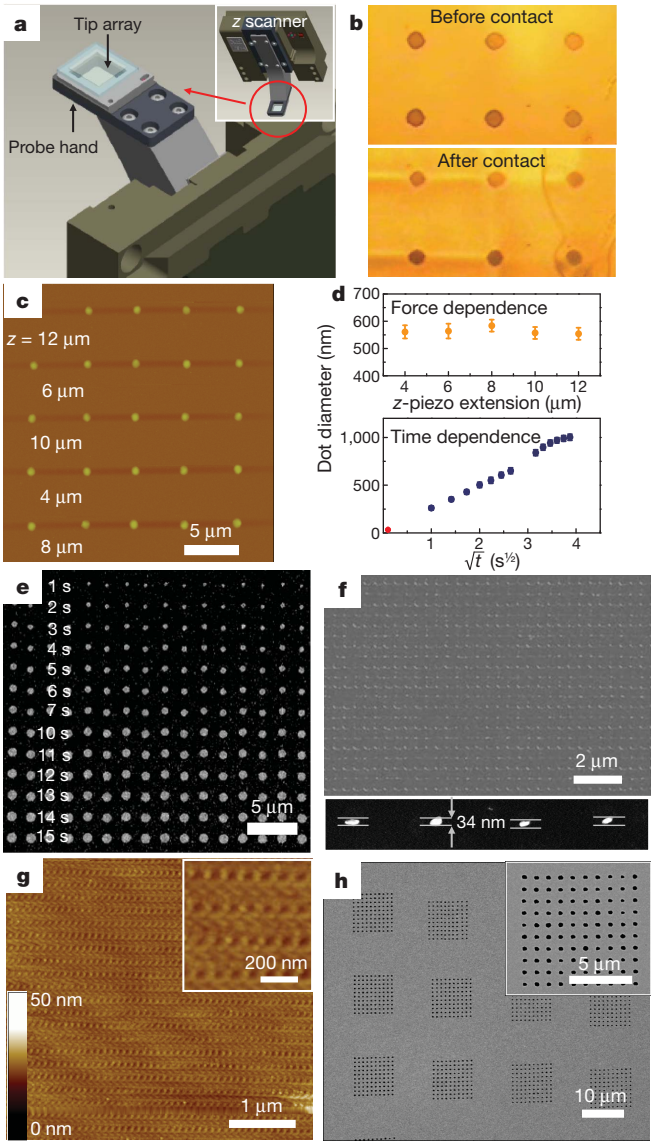

Figure 3 | Operating principles and single tip capabilities. **a**, A tip array attached to the probe hand of a 25-μm *z*-scanner that provides a 10 mm × 10 mm panning optical view for levelling the tips with a surface on the tilting stage. **b**, Optical images showing compression of the elastomer backing as the tips come in contact with the surface (see Supplementary Video 1). **c**, AFM image indicating the lack of force dependence of the PEG feature diameters when patterned onto a hexamethyldisilazane-coated Si surface with varying *z*-piezo extension and a constant dwell time of 0.5 s (humidity of 90%). The *z*-piezo extensions and measured diameters of the PEG dots are as follows: 12 μm, 554 ± 22 nm; 10 μm, 557 ± 22 nm; 8 μm, 584 ± 22 nm; 6 μm, 564 ± 27 nm; 4 μm, 561 ± 24 nm. **d**, Time and force dependence of feature size variation (orange dots from **c**, blue dots from **e**, and red dot from **f**). *t*, contact time. **e**, SEM image of a pattern of etched Au dots of different sizes on an Si surface created by intentionally varying the dwell time (shown in panel) of MHA-coated tips at a humidity of 50%. The time of MHA deposition and measured diameter of the Au dots are as follows: 15 s, 1,002 ± 32 nm; 14 s, 990 ± 30 nm; 13 s, 970 ± 28 nm; 12 s, 942 ± 30 nm; 11 s, 897 ± 30 nm; 10 s, 840 ± 31 nm; 7 s, 651 ± 31 nm; 6 s, 606 ± 29 nm; 5 s, 551 ± 31 nm; 4 s, 503 ± 28 nm; 3 s, 429 ± 24 nm; 2 s, 352 ± 22 nm; 1 s, 261 ± 22 nm. **f**, Main panel, SEM image of a pattern of etched Au dots on a Si surface patterned with a dwell time of 0.01 s and at a humidity of 15%. Inset (bottom), a magnified SEM image of the Au dots. **g**, Main panel, AFM topographical image of the dot pattern of PMMA prepared by indentation with a Si tip at room temperature. Inset, a magnified image. **h**, Main panel, SEM image of Au hole patterns created by Au etching after removing MHA SAM at a bias voltage of −5 V with a dwell time of 5 s and at a humidity of 30%. Inset, a magnified image.

©2011 Macmillan Publishers Limited. All rights reserved

holes at a pitch distance of 100 nm (Fig. 3g; see also Supplementary Fig. 4). To show that these tip arrays could also transfer electrical energy to a surface, the tip arrays were coated with Au (50 nm Au, 5 nm Ti adhesion layer), attached to a voltage source, and brought into contact with an Au surface coated with MHA[29]. Following the application of −5 V with a contact time of 5 s at a humidity of 30%, the MHA self-assembled monolayer (SAM) was removed selectively from the points where voltage had been applied, leaving an array of holes with an average diameter of 274 ± 20 nm (Fig. 3h).

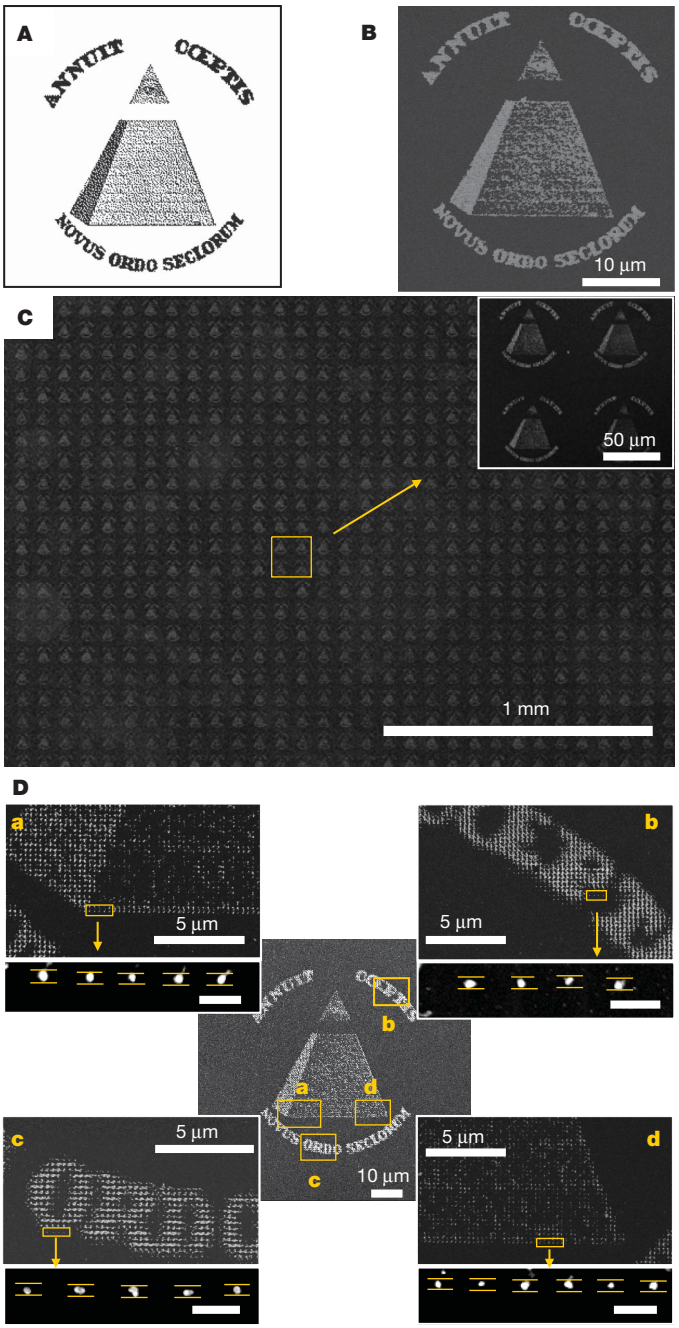

Figure 4 | High-resolution parallel HSL writing. **A**, Dot matrix map of the pyramid on the US $1 bank-note. The image consists of 6,982 dots. **B**, SEM image of the resulting etched Au pattern produced by writing the image with a dwell time of 0.01 s per dot at a humidity of 40%. The image size is 30 × 33 μm and the distance between dots is 150 nm (a large area pattern is shown in Supplementary Fig. 5). **C**, Main panel, SEM image of a representative region of ~ 19,000 duplicates of the pyramid from the US $1 bank-note. The size of each duplicate is 55 × 60 μm with a 270-nm dot-centre-to-dot-centre distance. Inset, magnified SEM image of four pyramid replicas. **D**, Central panel, SEM image of a single pyramid, 55 × 60 μm in size. Also shown are magnified images of the bottom-left corner of pyramid (**a**), the top-right letters 'OCEPTIS' (**b**), the bottom letters 'ORDO' (**c**), and the bottom-right corner of a pyramid (**d**). Each sub-panel **a**–**d** shows at bottom a magnified image of the marked regions with individual dots (41 ± 7 nm in diameter). Scale bars in sub-panel insets are 270 nm.

HSL is distinguished from all other lithographic techniques by the ability to form arbitrary patterns in massively parallel (over a 1-cm^2 area) and mask-less fashion at a feature resolution of less than 50 nm. The record for feature resolution with a cantilever array over a 1-cm^2 area still stands at 80 nm (ref. 8). The ability to generate arbitrary patterns with HSL tip arrays was evaluated in the context of reproducing a bitmap representation of the pyramid on the US $1 bank-note. The resolution limits of this first HSL tip array were also evaluated in this experiment. The pyramid image was loaded into the Park AFM custom XEL software, which converted the image into a dot-matrix representation. The computer generated pattern is composed of 6,982 dots with the corresponding position coordinates for each dot (Fig. 4A). The 4,750 HSL tip array (1 cm × 1 cm) was inked with MHA and then subsequently used to generate the etched Au dots (0.01 s contact time, 40% humidity) that comprise the pyramid and surrounding letters (Fig. 4B; see also Supplementary Fig. 6). In this initial proof-of-concept, the resulting etched Au pattern is an accurate miniaturized duplication (30 × 33 μm) of the bitmap image. Each dot is connected to the others in the structure to make the observed pyramid and letters (the intended pitch was 150 nm). In order to resolve individual dots, the image size was increased to 55 × 60 μm with a 270-nm dot pitch while maintaining the number of dots (6,982). The tip–substrate contact time was kept constant at 0.01 s but the humidity was lowered to 30% to decrease the molecule transport rate and, as a consequence, feature size. A representative portion of the ~19,000 replicas (yield >99%) generated across the 1-cm^2 substrate show the quality and high resolution of this novel nanofabrication technique (Fig. 4C). Importantly, at the edge of the etched Au patterns (Fig. 4D), individual dots can be clearly seen, allowing us to determine the average feature diameter (41 ± 7 nm across the 1-cm^2 area; Supplementary Fig. 7). The standard deviation of the etched Au dot diameters for features generated by HSL was 17% across the 1-cm^2 area, which is a combined result of minor variations in surface etching, tip morphology, ink coating, and the polycrystallinity of the Au surface. These results confirm that registry and levelling of the tip array are maintained within the field of view of each tip and between tips as well, showing the flexibility and robustness of this technique. The total time required to fabricate this large-area, high-resolution pattern (1.32×10^8 dots) was about 200 min with the custom Park XEL lithography software.

In conclusion, this is to our knowledge the first time a hard-tip-based approach has been realized in the context of a cantilever-free system, and it offers significant advantages in terms of resolution, scalability and decreased complexity compared to many previous approaches[30]. Importantly, the cost of each tip array is comparable to the cost of a single AFM tip, and the HSL approach could be implemented with the now common conventional AFM equipment.

METHODS SUMMARY

Si wafers (NOVA Electronic Materials; resistivity, 1–10 Ω cm, (100) orientation, 50 ± 5 μm thick) with a 10,000 Å (±5%) SiO_2 layer on each side were used for fabricating the tip arrays. For etch mask fabrication, the square mask along the <110> direction was transferred into the SiO_2 layer by photolithography with photoresist (AZ 1518, MicroChem) and isotropic etching with buffered hydrofluoric acid (HF, Transene) for 9 min. The sample was transferred to 40 wt % KOH solution at 75 °C and held in the centre of the etchant in a Teflon holder. It is worth noting that the use of the bottom SiO_2 layer contacting PDMS significantly increases the adhesion of tips to PDMS during etching. In a typical patterning experiment, HSL was performed with a Park System XE-150 AFM equipped with a tilt stage and an environmental chamber (that is, active humidity control) at a relative humidity of 15–50% and a temperature of ~25 °C. The statistics used to evaluate the patterned features are based on one standard deviation. A summary of the statistics is presented in Supplementary Fig. 8.

©2011 Macmillan Publishers Limited. All rights reserved

Full Methods and any associated references are available in the online version of the paper at www.nature.com/nature.

Received 30 August; accepted 24 November 2010.

1. Braunschweig, A. B., Huo, F. & Mirkin, C. A. Molecular printing. *Nature Chem.* **1,** 353–358 (2009).
2. Salaita, K., Wang, Y. & Mirkin, C. A. Applications of dip-pen nanolithography. *Nature Nanotechnol.* **2,** 145–155 (2007).
3. Quate, C. F. Scanning probes as a lithography tool for nanostructures. *Surf. Sci.* **386,** 259–264 (1997).
4. Tseng, A. A., Notargiacomo, A. & Chen, T. P. Nanofabrication by scanning probe microscope lithography: A review. *J. Vac. Sci. Technol. B* **23,** 877–894 (2005).
5. Rosa, L. G. & Liang, J. Atomic force microscope nanolithography: dip-pen nanoshaving, nanografting, tapping mode, electrochemical and thermal nanolithography. *J. Phys. Condens. Matter* **21,** 483001 (2009).
6. Saavedra, H. M. *et al.* Hybrid strategies in nanolithography. *Rep. Prog. Phys.* **73,** 036501 (2010).
7. Bullen, D. *et al.* Parallel dip-pen nanolithography with arrays of individually addressable cantilevers. *Appl. Phys. Lett.* **84,** 789–791 (2004).
8. Salaita, K. *et al.* Massively parallel dip-pen nanolithography with 55000-pen two-dimensional arrays. *Angew. Chem. Int. Edn* **45,** 7220–7223 (2006).
9. Vettiger, P. *et al.* Ultrahigh density, high-data-rate NEMS-based AFM data storage system. *Microelectron. Eng.* **46,** 11–17 (1999).
10. Vettiger, P. *et al.* The 'Millipede'—more than one thousand tips for future AFM data storage. *IBM J. Res. Dev.* **44,** 323–340 (2000).
11. Hong, S. H. & Mirkin, C. A. A nanoplotter with both parallel and serial writing capabilities. *Science* **288,** 1808–1811 (2000).
12. Zhang, M. *et al.* MEMS nanoplotter with high-density parallel dip-pen nanolithography probe arrays. *Nanotechnology* **13,** 212–217 (2002).
13. Salaita, K. *et al.* Sub-100 nm, centimeter-scale, parallel dip-pen nanolithography. *Small* **1,** 940–945 (2005).
14. Lenhert, S., Sun, P., Wang, Y. H., Fuchs, H. & Mirkin, C. A. Massively parallel dip-pen nanolithography of heterogeneous supported phospholipid multilayer patterns. *Small* **3,** 71–75 (2007).
15. Mirkin, C. A. The power of the pen: development of massively parallel dip-pen nanolithography. *ACS Nano* **1,** 79–83 (2007).
16. Eigler, D. M. & Schweizer, E. K. Positioning single atoms with a scanning tunneling microscope. *Nature* **344,** 524–526 (1990).
17. Leung, O. M. & Goh, M. C. Orientational ordering of polymer by atomic force microscope tip-surface interaction. *Science* **255,** 64–66 (1992).
18. Xia, Y. & Whitesides, G. M. Soft lithography. *Angew. Chem. Int. Edn* **37,** 550–575 (1998).
19. Gates, B. D. *et al.* New approaches to nanofabrication: molding, printing, and other techniques. *Chem. Rev.* **105,** 1171–1196 (2005).
20. Ginger, D. S., Zhang, H. & Mirkin, C. A. The evolution of dip-pen nanolithography. *Angew. Chem. Int. Edn* **43,** 30–45 (2004).
21. Kumar, A. & Whitesides, G. M. Features of gold having micrometer to centimeter dimensions can be formed through a combination of stamping with an elastomeric stamp and an alkanethiol ''ink'' followed by chemical etching. *Appl. Phys. Lett.* **63,** 2002–2004 (1993).
22. Zheng, Z., Jang, J.-W., Zheng, G. & Mirkin, C. A. Topographically flat, chemically patterned PDMS stamps made by dip-pen nanolithography. *Angew. Chem. Int. Edn* **47,** 9951–9954 (2008).
23. Piner, R. D., Zhu, J., Xu, F., Hong, S. H. & Mirkin, C. A. ''Dip-pen'' nanolithography. *Science* **283,** 661–663 (1999).
24. Hong, S. H., Zhu, J. & Mirkin, C. A. Multiple ink nanolithography: toward a multiple-pen nano-plotter. *Science* **286,** 523–525 (1999).
25. Huo, F. *et al.* Polymer pen lithography. *Science* **321,** 1658–1660 (2008).
26. Liao, X., Braunschweig, A. B. & Mirkin, C. A. ''Force-feedback'' leveling of massively parallel arrays in polymer pen lithography. *Nano Lett.* **10,** 1335–1340 (2010).
27. Liu, J., Betzner, T. M. & Henderson, H. T. Etching of self-sharpening {338} tips in (100) silicon. *J. Micromech. Microeng.* **5,** 18–24 (1995).
28. Yun, M. H., Burrows, V. A. & Kozicki, M. N. Analysis of KOH etching of (100) silicon on insulator for the fabrication of nanoscale tips. *J. Vac. Sci. Technol. B* **16,** 2844–2848 (1998).
29. Jang, J., Maspoch, D., Fujigaya, T. & Mirkin, C. A. A. ''Molecular eraser'' for dip-pen nanolithography. *Small* **3,** 600–605 (2007).
30. Nie, Z. & Kumacheva, E. Patterning surfaces with functional polymers. *Nature Mater.* **7,** 277–290 (2008).

Supplementary Information is linked to the online version of the paper at www.nature.com/nature.

Acknowledgements C.A.M. acknowledges the US Air Force Office of Scientific Research (AFOSR), the US Defense Advanced Research Projects Agency (DARPA) and the US NSF (NSEC program) for support of this research. C.A.M is grateful for a NSSEF Fellowship from the US Department of Defense. A.B.B is grateful for a NRSA fellowship from the US NIH. We thank Z. Zheng for discussions.

Author Contributions W.S. and C.A.M designed all experiments. W.S., A.B.B. and C.A.M contributed to this work in analysing results and drafting the manuscript. W.S., A.B.B., X.L., J.C., J.K.L. and G.Z. also performed experiments and helped with revisions.

Author Information Reprints and permissions information is available at www.nature.com/reprints. The authors declare no competing financial interests. Readers are welcome to comment on the online version of this article at www.nature.com/nature. Correspondence and requests for materials should be addressed to C.A.M. (chadnano@northwestern.edu).

©2011 Macmillan Publishers Limited. All rights reserved

METHODS

Fabrication of the Si etching masks. Si wafers (NOVA Electronic Materials; resistivity 1–10 Ωcm, (100) orientation, 50 ± 5 μm thick) with a 10,000-Å (±5%) SiO_2 layer on each side were used for fabricating the tip arrays. The wafers were cleaned in acetone, ethanol, then rinsed with water before use. In preparing the elastomer base, PDMS and a curing agent (Sylgard 184 Silicone) were mixed in 20:1 ratio (w/w), and then degassed under vacuum (10^{-3} torr). Oxygen-plasma-treated (1 min at 60 W at a pressure of 100 mtorr) wafers were then placed on uncured PDMS on clean glass slides, followed by curing at 70 °C for 24 h. This wafer/PDMS/glass slide sample is easier to handle and less fragile than the 50-μm-thick wafer alone. The choice of a particular mask material depends on a number of considerations. The main issues are availability of materials, ease of the process (processing time, complexity of the process, and reliability), and selectivity of the etching process. Metals such as Au, Cr, Pt, Ag, Cu and Ti are known to be resistant to KOH etching. In our case, however, thermally evaporated Au/Ti was used as an etching mask and found to be vulnerable to KOH degradation. Indeed, the use of an Au (500 nm)/Ti (100 nm) mask (instead of SiO_2) followed by KOH etching for 1 h at 75 °C resulted in a significant failure in tip fabrication due to pinholes in the mask. Thermally grown SiO_2 is a better mask material as it provides a greater etching selectivity than many metal materials with respect to Si (of the order of 500:1). As the etching rate of Si (100) in 40 wt% KOH at 75 °C is 50 μm h^{-1}, the minimum required thickness of SiO_2 is 250 nm for an experimentally viable fabrication procedure, which justifies the use of the 1-μm-thick SiO_2 coating. For etch mask fabrication, the square mask along the <110> direction was transferred into the SiO_2 layer by photolithography with photoresist (AZ 1518, MicroChem) and isotropic buffered hydrofluoric acid (9% HF, Transene) etch for 9 min. To remove the photoresist, the wafer was cleaned in acetone, then ethanol, and subsequently dried with flowing nitrogen. The wafer was finally cleaned in an oxygen plasma. These cleaning procedures before Si etching were found to improve the uniformity of the tips (1 min at 60 W at a pressure of 100 mtorr).

Fabrication of Si tip arrays. Following photolithography, the wafer was etched for 1 min using ammonium fluoride (20% NH_4F, Time Etch, Transene) to remove the native oxide from the surface of the Si regions, which was followed by rinsing in water and drying with a nitrogen stream. The sample was immediately transferred to 40 wt% KOH solution at 75 °C and held in the centre of the etchant in a Teflon holder. The solution was continuously stirred to reduce the effect of micro-masking by hydrogen bubbles generated in the reaction at the Si surface. After 60–65 min, the sample was removed from the etchant, rinsed in water and dried under a nitrogen stream. It is worth noting that the use of the bottom SiO_2 layer contacting PDMS significantly increases the adhesion of tips to PDMS during etching. For example, it was observed that a number of tips fell off of the PDMS surface during etching when no interfacial SiO_2 layer was used (Supplementary Fig. 1).

Fabrication of nanopatterns by material and energy delivery. In a typical experiment, HSL was performed with a Park System XE-150 AFM equipped with a tilt stage and an environmental chamber (that is, active humidity control, error range ~5%) at a relative humidity of 15–80% and a temperature of ~23–26 °C. Environmental parameters that affect feature size include relative humidity, temperature, substrate, and ink concentration. In the temperature range of 23–26 °C, MHA transport from a tip to a surface is less sensitive to temperature. The arrays were driven by the custom XEL lithography software (Park System) capable of controlling the position, dwell time, and *z*-piezo extension at every point in an arbitrary pattern. To pattern MHA (Sigma-Aldrich) on an Au surface, MHA (5–10 mM) was spin-coated (1 ml, 1,000 r.p.m., 30 s) onto an oxygen-plasma-cleaned HSL tip array (1 min). The tip array was aligned with respect to the surface by varying the tilt of the surface until all tips were observed by optical microscopy to contact the surface on *z*-piezo extension. The inked Si tip array was used for generating MHA dot patterns on a thermally evaporated polycrystalline Au surface (20–25 nm Au with a 5 nm Ti adhesion layer coated on Si) by bringing the tip array repeatedly into contact with the Au surface. The exposed Au on this MHA patterned surface was subsequently etched (the substrate was immersed in 20 mM thiourea (aq.), 30 mM $FeNO_2$ (aq.), 20 mM HCl (aq.), and 2 mM octanol (aq.) and gently shaken by hand) for 4–5 min to yield raised structures that are approximately 20–25 nm in height and easily imaged by SEM (3–5 kV in SE mode at a pressure of 10^{-5} torr; Hitachi S4800). Before imaging the etched Au features, the MHA SAM was removed by oxygen plasma. We inspected the Au surface (20-nm thick on 5-nm thick Ti) before patterning and after patterning and etching (Supplementary Fig. 9). To pattern PEG, a 5 mg ml^{-1} poly(ethylene glycol) (PEG) solution (M_w = 2,000) was prepared in pure ethanol and sonicated at room temperature for 10 min until the PEG dissolved. The tip array was cleaned by oxygen plasma for 1 min at 60 W at a pressure of 100 mtorr. 1 ml of the PEG solution was dropped onto the tip array and allowed to settle for 1 min before spin coating at 1,000 r.p.m. for 1 min. The tip array was mounted onto the patterning platform and then levelled. The environmental chamber was sealed, and a humidifier was used to increase the relative humidity to at least 80%. To pattern nano-holes by the transfer of mechanical energy, PMMA (495 PMMA C3, MicroChem) diluted in chlorobenzene (1 g PMMA: 2.5 g chlorobenzene) was spin-coated onto the Si substrate at 3,000 r.p.m. for 45 s, and thermally annealed at 180 °C for 1 min. The thickness of the resulting film was 31 ± 3 nm, and the surface roughness (r.m.s. value) was about 1.1 ± 0.4 nm. Patterns were generated by indentation of the film by the tip array at room temperature by controlling the position and extension of the *z*-piezo scanner. After patterning, the surface roughness was about 1.30 ± 0.05 nm and peak-to-peak roughness (highest point minus lowest point) was about 11.69 ± 0.99 nm. To electrically pattern nano-holes, the Si tip array was first coated with Au (50 nm) / Ti (5 nm) to become conductive. SAMs of MHA molecules were prepared on Au thin films by immersing the substrate in a 1 mM ethanolic MHA solution for 1 h, followed by rinsing with ethanol and water, and drying with nitrogen. An Au-coated Si tip array with a bias voltage of –5 V contacted the MHA SAM surface to selectively desorb portions of the MHA SAM surface under ambient conditions (~30% humidity, 23 °C). The resulting indentations were characterized by topographical AFM.

©2011 Macmillan Publishers Limited. All rights reserved

Reproduced with permission of the copyright owner. Further reproduction prohibited without permission.